

## FEMTOSCOPY APPLICATION OF THE NEW EPOS MODEL TO THE STAR EXPERIMENT

*K. Mikhailov*<sup>a</sup>, *K. Werner*<sup>b</sup>, *Iu. Karpenko*<sup>b,c</sup>, *T. Pierog*<sup>d</sup>

<sup>a</sup> Institute for Theoretical and Experimental Physics, Moscow

<sup>b</sup> SUBATECH, University of Nantes — IN2P3/CNRS — EMN, Nantes, France

<sup>c</sup> Bogolyubov Institute for Theoretical Physics, Kiev

<sup>d</sup> Forschungszentrum Karlsruhe, Institut für Kernphysik, Karlsruhe, Germany

The space-time structure at hadronization was studied within new EPOS model using femtoscopy methods. The results of the study was compared with the STAR HBT data for AuAu collision and first ALICE HBT data for  $pp$  collisions. The model-predicted  $m_T$  and centrality dependence of  $R_{out}$ ,  $R_{side}$  and  $R_{long}$  femtoscopy parameters were found to be in accordance with the STAR data.

PACS: 25.75.-q

### INTRODUCTION

In this paper, we present an application of the new EPOS model [1,2] to the femtoscopy results of STAR and ALICE experiment. New EPOS model is a realistic treatment of the hydrodynamic evolution of ultrarelativistic heavy-ion collisions, based on the following features: initial conditions obtained from a flux tube approach (EPOS), compatible with the string model used since many years for elementary collisions (electron–positron, proton–proton), and the color glass condensate picture; consideration of the possibility to have a (moderate) initial collective transverse flow; event-by-event procedure, taking into account the highly irregular space structure of single events, being experimentally visible via the so-called ridge structures in two-particle correlations; core–corona separation, considering the fact that only part of the matter thermalizes; use of an efficient code for solving the hydrodynamic equations in  $3 + 1$  dimensions, including the conservation of baryon number, strangeness, and electric charge; employment of a realistic equation of state, compatible with lattice gauge results with a cross-over transition from the hadronic to the plasma phase; use of a complete hadron resonance table, making our calculations compatible with the results from statistical models; hadronic cascade procedure after hadronization from the thermal system at an early stage.

### FEMTOSCOPY

A direct insight into the space-time structure at hadronization is obtained from using femtoscopy methods [3,7], where the study of two-particle correlations provides information about the source function  $S(\mathbf{P}, \mathbf{r}')$ , being the probability of emitting a pair with total momentum  $\mathbf{P}$  and relative distance  $\mathbf{r}'$ . Under certain assumptions, the source function is related to the measurable two-particle correlation function  $C(\mathbf{P}, \mathbf{q})$  as

$$C(\mathbf{P}, \mathbf{q}) = \int d^3 \mathbf{r}' S(\mathbf{P}, \mathbf{r}') |\Psi(\mathbf{q}', \mathbf{r}')|^2, \quad (1)$$

where  $\mathbf{q}$  is the relative momentum and  $\Psi$  is the outgoing two-particle wave function, with  $\mathbf{q}'$  and  $\mathbf{r}'$  being relative momentum and distance in the pair center-of-mass system. The source function  $S$  can be obtained from our simulations; concerning the pair wave function, we follow [8]. As an application, we investigate  $\pi^+-\pi^+$  correlations. Here, we only consider quantum statistics for  $\Psi$ , no final state interactions, to compare with Coulomb corrected data. To compute the discretized correlation function  $C'_{ij} = C(\mathbf{P}_i, \mathbf{q}_j)$ , we do our event-by-event simulations, and compute for each event  $C'_{ij} = \sum_{\text{pairs}} |\Psi(\mathbf{q}', \mathbf{r}')|^2$ , where the sum extends over

all  $\pi^+$  pairs with  $\mathbf{P}$  and  $\mathbf{q}$  within elementary momentum-space volumes at respectively  $\mathbf{P}_i$  and  $\mathbf{q}_j$ . Then we compute the number of pairs  $N_{ij}$  for the corresponding pairs from mixed events, being used to obtain the properly normalized correlation function  $C_{ij} = C'_{ij}/N_{ij}$ . The correlation function will be parameterized as

$$C(\mathbf{P}, \mathbf{q}) = 1 + \lambda \exp(-R_{\text{out}}^2 \mathbf{q}_{\text{out}}^2 - R_{\text{side}}^2 \mathbf{q}_{\text{side}}^2 - R_{\text{long}}^2 \mathbf{q}_{\text{long}}^2), \quad (2)$$

where «long» refers to the beam direction, «out» is parallel to projection of  $\mathbf{P}$  perpendicular to the beam, and «side» is the direction orthogonal to «long» and «out» [9–11]. In Fig. 1, we show the results for the fit parameters  $\lambda$ ,  $R_{\text{out}}$ ,  $R_{\text{side}}$ , and  $R_{\text{long}}$ , for five different centrality classes and for four  $k_T$  intervals defined as (in MeV):  $\text{KT1} = [150, 250]$ ,  $\text{KT2} = [250, 350]$ ,  $\text{KT3} = [350, 450]$ ,  $\text{KT4} = [450, 600]$ , where  $k_T$  of the pair is defined as

$$k_T = \frac{1}{2}(|\mathbf{p}_T(\text{pion 1}) + \mathbf{p}_T(\text{pion 2})|). \quad (3)$$

The results are plotted as a function of  $m_T = \sqrt{k_T^2 + m_\pi^2}$ . The model describes well the radii, the experimental lambda values are slightly below the calculations, maybe due to particle

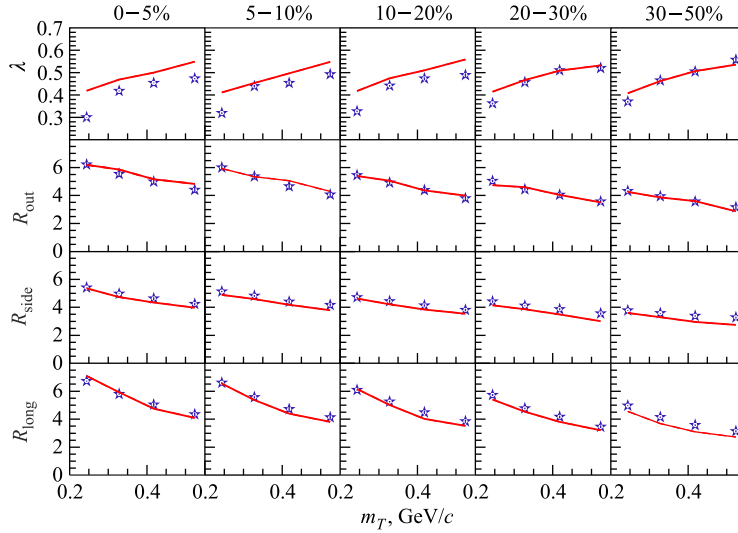


Fig. 1. Femtoscopy radii  $R_{\text{out}}$ ,  $R_{\text{side}}$ , and  $R_{\text{long}}$ , as well as  $\lambda$  as a function of  $m_T$  for different centralities (0–5% most central, 5–10% most central, and so on). The solid lines are the full calculations (including hadronic cascade), the stars data [12]

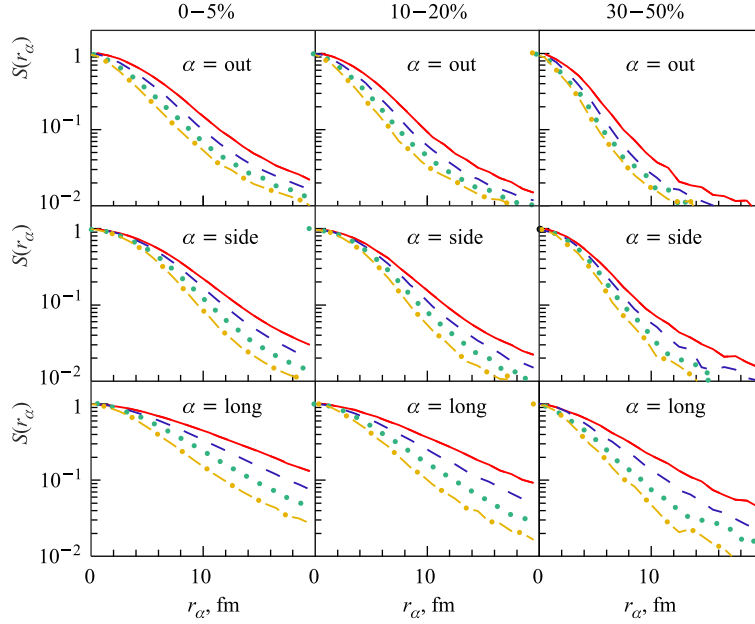


Fig. 2. The source functions as obtained from our simulations, for three different centralities (0–5% most central, 10–20% most central, and 30–50% most central), representing the distribution of the space separation of the emission points of the pairs, in the «out»–«side»–«long» coordinate system, in the longitudinal comoving frame. The different curves per plot correspond to the different  $k_T$  bins, see text

misidentification. Concerning the  $m_T$  dependence of the radii, we observe the same trend as seen in the data [12]: all radii decrease with increasing  $m_T$ , and the radii decrease as well with decreasing centrality. This can be traced back to the source functions, shown in Fig. 2. These source functions are by definition the distributions of the distances  $x_i$  (pion 1) –  $x_i$  (pion 2) of the pairs, where  $x_i$  are coordinates of the emission points. We use the «out»–«side»–«long» coordinate system, and the longitudinal comoving reference frame. To account for the fact that only small values of the magnitude of the relative momentum  $|\mathbf{q}|$  provide a nontrivial correlation, we only count pairs with  $|\mathbf{q}| < 75$  MeV. The different curves per plot correspond to the different values of  $k_T$  bins: the upper curve (solid) corresponds to KT1, the second curve from the top (dashed) corresponds to KT2, and so on. In other words, the curves get narrower with increasing  $k_T$ , which is perfectly consistent with the decreasing radii in Fig. 1. Concerning the centrality dependence, the curves get narrower with decreasing centrality, in agreement with decrease of radii with decreasing centrality seen in Fig. 1.

The fitting procedure used to obtain the femtoscopic radii is based on the hypothesis that the source functions are Gaussians, the fit is therefore blind concerning the non-Gaussian tails. Due to the fact that the source function from the complete calculations and the full thermal scenario are identical apart from the tails, we expect similar results for these two scenarios, whereas the calculation without cascade should give smaller radii. This is exactly what we observe in Fig. 3, where we show femtoscopic radii for the calculations without hadronic cascade (solid line) and with hydrodynamical evolution till final freeze-out at 130 MeV (dashed). We observe always a decrease of the radii with  $m_T$ , but the dependence is somewhat weaker as compared to the data. But the magnitude in case of no cascade is very

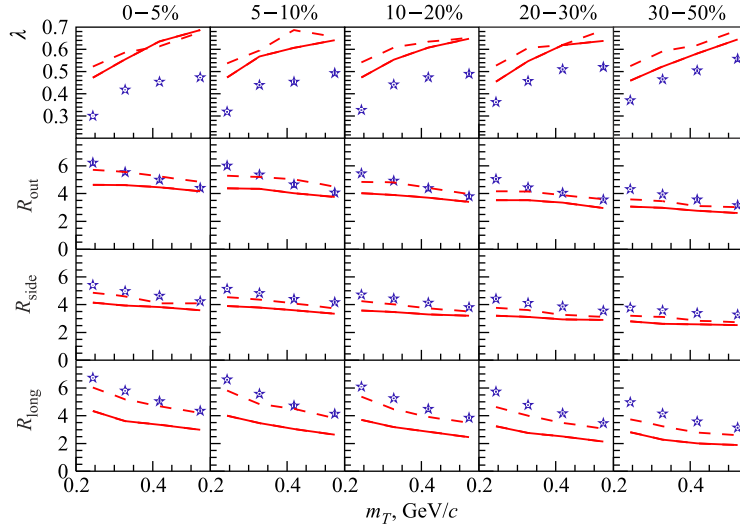


Fig. 3. The same as in Fig. 1, but the calculations are done without hadronic cascade (solid line) or with a hydrodynamic evolution through the hadronic phase with freeze-out at 130 MeV (dashed)

low compared to the two other scenarios, which are relatively close to each other, and to the data. Here the radii do not allow one to discriminate between two scenarios which have nevertheless quite different source functions. This is a well-known problem, and there are methods to go beyond Gaussian parameterizations [13–17], but we will not discuss this any further.

Although the Gaussian parameterizations represent only an incomplete information about the source functions, the centrality and transverse momentum dependence of the radii is nevertheless very useful. It is a necessary requirement for all models of soft physics to describe these radii correctly. There has been for many years an inconsistency, referred to as HBT puzzle [18]. Although hydrodynamics describes very successfully elliptical flow and to some extent particle spectra, one cannot get the femtoscopic radii correctly, when one uses simple hydrodynamics. Using transport models (and an event-by-event treatment) may help [6]. In [18], it has been shown that the puzzle can actually be solved by adding pre-equilibrium flow, taking a realistic equation of state, adding viscosity, using a more compact or more Gaussian initial energy density profile, and treating the two-pion wave function more accurately. It has also been shown [19] that using a Gaussian initial energy density profile, an early starting time (equivalent to initial flow), and a cross-over equation of state, and a late sudden freeze-out (at 145 MeV) helps to describe the femtoscopic radii, and to some extent the spectra. The scenario in [19] is compatible with our scenario hydrodynamical evolution till final freeze-out at 130 MeV, which allows us to get the femtoscopic radii correctly (see Fig. 3).

K.M. acknowledges partial support by the RFBR-CNRS grants No.08-02-92496-NTsNIL\_a and No.10-02-93111-NTsNIL\_a.

#### REFERENCES

1. Werner K. et al. // Phys. Rev. C. 2010. V. 82. P. 044904; nucl-th/1004.0805.
2. Werner K. et al. nucl-th 1010.0400.

3. *Kopylov G. I., Podgoretsky M. I.* // *Sov. J. Nucl. Phys.* 1972. V. 15. P. 219.
4. *Kopylov G. I., Podgoretsky M. I.* // *Sov. J. Nucl. Phys.* 1974. V. 18. P. 336.
5. *Pratt S.* // *Phys. Rev. Lett.* 1984. V. 53. P. 1219–1221.
6. *Lisa M. A. et al.* // *Ann. Rev. Nucl. Part. Sci.* 2005. V. 55. P. 357–402.
7. *Kisiel A., Florkowski W., Broniowski W.* // *Phys. Rev. C.* 2006. V. 73. P. 064902.
8. *Lednický R.* // *Part. Nucl.* 2009. V. 40. P. 307.
9. *Bertsch G. F., Gong M., Tohyama M.* // *Phys. Rev. C.* 1988. V. 37. P. 1896.
10. *Pratt S.* // *Phys. Rev. D.* 1986. V. 33. P. 1314.
11. *Chapman S., Scotto P., Heinz U. W.* // *Phys. Rev. Lett.* 1995. V. 74. P. 4440.
12. *Adams J. et al.* // *Phys. Rev. C.* 2005. V. 71. P. 44906.
13. *Verde G. et al.* // *Phys. Rev. C.* 2002. V. 65. P. 054609.
14. *Panitkin S. Y. et al.* // *Phys. Rev. Lett.* 2001. V. 87. P. 112304.
15. *Brown D. A., Danielewicz P.* // *Phys. Rev. C.* 2001. V. 64. P. 014902.
16. *Brown D. A., Wang Fu-qiang, Danielewicz P.* // *Phys. Lett. B.* 1999. V. 470. P. 33–38.
17. *Pratt S.* // *Nucl. Phys. A.* 2009. V. 830. P. 51C–57C.
18. *Chung P. et al.* // *Phys. Rev. Lett.* 2003. V. 91. P. 162301.
19. *Florkowski W. et al.* // *Nucl. Phys. A.* 2009. V. 830. P. 821c–824c.